Fifth International Symposium on Marine Propulsors
smp'17, Espoo, Finland, June 2017

Application of multi-objective optimization based design to high-speed craft propellers

Stefano Gaggero[1], Giorgio Tani[1], Diego Villa[1], Michele Viviani[1], Pierluigi Ausonio[2], Piero Travi[2], Giovanni Bizzarri[3], Francesco Serra[3]

[1]University of Genoa, Department of Electrical, Electronic, Telecommunications Engineering and Naval Architecture, Genoa, Italy
[2]DETRA Custom Propellers Genoa, Italy
[3]Azimut|Benetti Group, Varazze, Italy

ABSTRACT

The design of a propeller for a high-speed craft is addressed by using a multi-objective numerical optimization approach. By combining a fast and reliable Boundary Elements Method, a viscous flow solver based on the RANSE approximation, a parametric 3D description of the blade and a genetic algorithm, the new propeller shape is designed to improve the propulsive efficiency, reduce the cavitation extension, increase the cavitation inception speed and maximize, at the same time, the ship speed. Rather than by constraining the propeller delivered thrust, indeed, the proposed procedure works together with an engine-propeller matching algorithm that, each time a new propeller is defined, identifies the achievable maximum speed and the resulting engine functioning point that turn in additional goals for the optimization. A set of optimal propellers, obtained through the design by optimization based on potential flow calculations, are preliminary selected for additional viscous analyses in order to further validate the results of the BEM calculations and provide a deeper insight into the complex flow fields of high-speed propellers useful for choosing the optimal geometry. The improvements observed at the cavitation tunnel and the substantial increase of the maximum ship speed during sea trials on a high-speed craft provided by Azimut|Benetti prove the reliability of the design procedure.

Keywords

High-Speed Propeller, Multi-objective Optimization, BEM, RANSE, Cavitation.

1 INTRODUCTION

The state of the art of fast propeller design codes is commonly based on classical vortical theories. These methods, all derived by the vortex line theory of Lerbs (1952) with surface exact or approximated corrections, have been used and adapted in many propeller design codes. Grossi (1980) developed, for instance, a lifting surface code that is routinely adopted for the propeller preliminary design of many of the Fincantieri Group ships while, recently Diniz and Brizzolara (2015), Brizzolara et al. (2013) and Brizzolara et al. (2012) have applied a similar approach for counter-rotating propellers.

A significant step towards the design of highly-loaded or unconventional geometries was represented by the variational approach by Kerwin et al. (1986) and by Coney (1989), extensively adopted for the design of different types of propellers also under severe working conditions. Anyhow, most of the effort was aimed to develop classical design strategies for the purpose of achieving the highest efficiency for a given thrust and only recently, Epps et al. (2011) extended the variational approach to consider simultaneously efficiency and cavitation performance at the endurance speed design point and at maximum speed off-design point, setting chord lengths and thickness to prevent cavitation at both operational conditions by using nested design loops.

All these approaches do take into account important design constraints, such as inception of cavitation and structural strength. However, the crude simplifications contained in these methods make them often insufficiently accurate, in case of modern fast propellers geometries having, for example, highly skewed blades, non-conventional profiles or mixed type of cavitation. Typically, the chord distribution is optimized for the design speed with some margin to prevent off-design cavitation that is only considered a posteriori, with some modifications to mitigate its negative influence in high-speed operations. On the contrary, the combination of chord and thickness should be better set through the design process to a minimum able to maximize efficiency and still prevent cavitation (sheet and midchord bubbles) in correspondence to any of the functioning conditions under investigation. In addition, the usual design tables of Brockett (1966) or the curve envelopes of the minimum pressure coefficient generally are not suitable when multiple design points are considered, when unconventional profile shapes are employed or when wide chord at tip are preferred. Moreover, neglecting (or approximating) the influence of the blade thickness may represent a serious drawback of a traditional lifting line/lifting surface approach in dealing

with off-design conditions that may involve midchord bubble cavitation. Cavitation and unsteadiness, indeed, play the most important role in the design of high performance propellers for high-speed boats. In these vessels, propellers are often subjected to strong non-uniform inflow and the unsteady cavitation could reduce their performance, in addition to the risk of corrosion and induced noise and vibrations that certainly have to be minimized in the case of pleasure yachts. These requirements definitely require more advanced design tools, based on (more) accurate flow solvers and able to deal with the multi-objective nature of each new innovative design.

Among the potential based theories, Boundary Elements Methods (BEM) have inherent better abilities to capture the thickness effect of the blade, of the hub and, eventually, also the effect of cavitation. Panels discretizing the surfaces are placed on the real geometry rather than on simplified and approximated representations as in the case of usual low fidelity methods like lifting line/lifting surface design approaches and the inclusion of the influence of the thickness is, for instance, of particular importance when monitoring the risk of bubble midchord cavitation. The method developed at the University of Genoa (Gaggero et al. 2010), similarly to those developed by different research groups (Fine, 1992, Fine and Kinnas, 1993, Vaz, 2005) can effectively predict the steady and the unsteady flow around the propeller with sheet cavitation, including supercavitation. Nevertheless all such models, which capture (and hence require in turn) more detailed information about the propeller geometry, cannot be directly integrated into a direct design procedure, differently from the simpler ones previously cited and, in fact, they are often used for validation of a given propeller design. Their level of accuracy is close to RANSE solvers (Brizzolara et al., 2008, Gaggero et al. 2010) at the design point while in very off-design conditions some discrepancies may be observed (Gaggero et al. 2014) but their computational efficiency is particularly high, allowing their systematic application in an inverse design process. A parametric optimization procedure represents, actually, the ideal application of BEMs for the design of such specific propellers, allowing for a more congruent and effective search of the best geometry subjected to more strict constraints and requirements. Into an optimization procedure, which can systematically change the main geometric parameters of the blades to converge on the multi-objective optimum Pareto solution, Boundary Elements Methods can be directly employed as they had been developed for, namely as analysis methods, taking advantages of all their specific peculiarities. In addition, population-based algorithms can natively handle multi-objective optimization tasks, overcoming the well-known limitations of gradient-based searching algorithms and they can exploit the computational efficiency of the BEMs for the evaluations of the thousands of solutions required for the Pareto convergence.

Such applications have been successfully carried out in the case of conventional and unconventional propellers. Bertetta et al. (2012) designed a controllable pitch propeller using a panel method, a robust parametric description of the blade geometry and an evolutionary algorithm of genetic type to define a geometry, whose requirements were to maximize efficiency and reduce the cavity extension in correspondence to two very different operative speeds achieved by changing the propeller pitch. Similarly (Gaggero et al. 2012), the same approach was adjusted in order to deal with ducted propellers and some improvements of an already well-designed propulsor based on the decelerating duct concept were even obtained. More recently (Gaggero et al. 2016a), the design by optimization based on BEM calculations led to significant improvements of the performance of Contracted and Tip Loaded propellers and set the state of the art for the design of a new class of tip loaded propellers (Gaggero et al. 2016b) with particular emphasis on cavitating tip vortexes and induced pressure pulses. In this latter case, the need of a robust parametric description of the unconventional blade geometry arose as a key point of the design process to avoid unrealistic improvements from unfeasible shapes.

In the present paper, an example of the application of the design by optimization to a high-speed boat propeller is given. The attention is focused on the optimization (maximization of efficiency and reduction of cavitation) of a custom propeller for a 95 feet high-speed craft manufactured by Azimut|Benetti designed with a traditional lifting surface approach. The objectives (or the constraints) on cavitation need to be revised in the light of the working conditions of such kind of high-speed propellers. Rather than requiring the minimization of the predicted cavity extension (or volume) or a sort of "advanced cavity constraints" like those successfully proposed by Vestig et al. (2016), a simpler analysis of the non-cavitating pressure distributions over the blade has been preferred. The minimization of the cavity extension, indeed, was successful in the case of conventional and unconventional geometries (Bertetta et al. 2012, Gaggero et al. 2016a, 2016b) but, in those cases, the propellers were subjected mainly to leading edge sheet cavitation that is the kind of cavitation Boundary Elements Methods can effectively deal with. High-speed propellers, generally, are from moderately to highly loaded and the higher value of the expanded blade area, while preventing severe suction pressure at the leading edge, flattens the pressure distribution and increases the risk of michord bubble cavitation. A design by optimization based on the minimization, among the others, of the midchord bubble extension seems questionable in the light of the further approximations to be accepted within the Boundary Elements Methods to deal with this phenomenon. A simple avoidance objective (or maximization of the margin against midchord cavitation), on the contrary, seems more reliable and, being based on simpler non-cavitating calculations, even more computationally efficient. At the leading edge similar non-cavitating based criteria may

successfully be derived to monitor the development of sheet cavitation too. RANSE calculations, in the light of the complexity of the flow around this kind of propellers, are, therefore, more than necessary, but their direct application as design tools in the optimization workflow, due to their comparatively lower computational efficiency is, at this moment, unfeasible. Consequently, viscous calculations in addition to measurements on a reference propeller, serve to validate the BEM, highlighting possible drawbacks and limitations to be opportunely addressed within the optimization process and, moreover, to reinforce the selection of the optimal propeller on the basis of calculations of only a reduced set of geometries from the Pareto convergence of the optimization process.

From a geometrical point of view, the design considers the widest possible variation of the main characteristics of the propeller in order to explore, within the prescribed constraints of structural strength, unconventional combinations of camber, pitch, sections mean line and chord. In addition, a different rake distribution from the one of the reference geometry is proposed. The reference rake distribution, pointing towards the suction side, was originally selected to increase the propeller efficiency at the cost of lower margin in cavitation inception (Dang, 2004). The new rake distribution, pointing instead towards the pressure side, effectively works to postpone the cavity inception, at the cost however of a less significant increase in propeller efficiency. Optimization, also for this specific issue, may represent a convenient way to design a better balanced geometry, increasing its efficiency with the same margin against cavitation when the rake points to the pressure side. The dedicated sea trials, discussed at the end of the paper, finally confirm the reliability and the effectiveness of this design approach.

All these activities have been carried out in the context of a cooperative project among Azimut|Benetti, DETRA Custom Propellers and the University of Genoa. Azimut|Benetti provided the information about the boat, supervised the project and its main guidelines, while the propeller design was carried out in cooperation between the University of Genoa and DETRA, which also manufactured the full-scale propellers. These activities have been partially funded by the MiSE – Ministero dello Sviluppo Economico, within the ABC (Advanced Boat Concept) Project – (Progetto n. C01/0889/00/X19 - Decreto di concessione del MiSE 02308 del 23 dicembre 2013).

2 TEST CASE: THE AZIMUT AZ95RPH CRAFT

A 95 feet length ship has been used as test case. The ship shown in Figure 1, built by Azimut|Benetti group, is a pleasure craft with a maximum speed of about 26 kn. The ship is equipped with two diesel engines (MTU 16V 2000M84, MTU, 2012) delivering a continuous maximum power of 1630kW each at 2450 rpm, with two propellers in twin-screw configuration. The main ship data are summarized in Table 1 while Table 2 summarizes the functioning conditions obtained from ship self-propulsion tests that will be assumed as reference for numerical and cavitation tunnel measurements. Due to confidentiality reasons, other data of the boat cannot be disclosed.

Figure 1: The Azimut 95 RPH high-speed pleasure craft.

Table 1: Main boat characteristics.

Ship	Azimut 95 RPH
Design Speed	>26 kn
Length	95 feet (28.956 m)
N° Engine	2
Engine Type	MTU 16V 2000M84
N° Propellers	2
Propeller design cavitation index σ_N	0.8463

Table 2: Propeller functioning conditions based on self-propulsion measurements.

Speed [kn]	K_T	σ_N
21	0.247	1.16
24	0.228	1
>26 (design)	0.212	0.86

3 NUMERICAL TOOLS BEHIND THE DESIGN BY OPTIMIZATION

The design by optimization, developed in this paper, relies on the application of different numerical tools. A Boundary Elements Method, developed at the University of Genoa, is adopted to efficiently evaluate the propellers performance within the optimization process. The commercial viscous flow solver StarCCM+ (CD-Adapco, 2012) serves to validate the optimal blade shape candidates and to have a further insight into the complex flow features around the propellers. An optimization framework (Esteco, 2014) drives the entire design process, thanks to a parametric description of the geometry, to convergence against selected objectives and constraints. A brief overview of these codes is summarized in the following sections.

3.1 Flow Solvers: BEM and RANSE

The current implementation of the BEM is based on the original formulation of Morino and Kuo (1974) in terms of perturbation velocity potential and Dirichlet boundary conditions. The key blade approach proposed Hsin (1990)

is adopted in the case of unsteady calculations (spatial non-uniform inflow or inclined shaft) while the partially nonlinear formulation of Fine and Kinnas (1993) and Fine (1992) solves the sheet cavitation bubble on both suction and pressure sides. Midchord bubble cavitation is partially accounted as a fictitious sheet cavity by the Villat-Brillouin criteria, as proposed by Mueller and Kinnas (1999). The reliability of the implementation has been verified through several benchmarks and applications, including unconventional and ducted propellers, with overall results in line with those provided by similar codes developed by other institutions and research groups. Based on these benchmarks and sensitivity analyses, calculations were carried out throughout the design by optimization process with a surface mesh consisting in 1500 hyperboloidal panels per blade and, in the case of unsteady calculations, with a time step equivalent to an angular increment of 6°. This setup proved to be a reasonable balance between accuracy and computational efficiency for an inverse design process. An example of the panel arrangement over the reference propeller is shown in Figure 2.

The inherent approximations introduced by the potential flow assumption prevent the application of the BEM for a reliable analysis of the propeller in off-design conditions. In addition, if for the design by optimization only the relative merits of one geometry with respect to the other (and not its absolute performance) may be sufficient for the selection of the optimal configurations, the characterization of the final performance of a propeller requires high-fidelity calculations, like those provided by RANSE solvers. In the present application, the finite volume solver StarCCM+ has been applied to overcome some of the limitations of the panel method and have a further guidance for the selection of the optimal propellers, considering both open water (steady) non-cavitating calculations and unsteady (inclined shaft) analysis with and without cavitation.

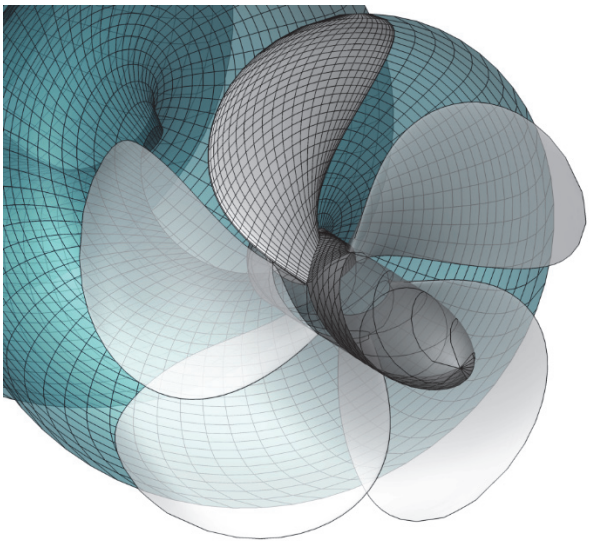

Figure 2: Surface mesh arrangement for the reference propeller for BEM calculations with the key blade highlighted.

An unstructured polyhedral mesh was selected for all the calculations. Details about the boundary conditions, the most appropriate arrangement of mesh refinements and prism layers may be found in Gaggero et al. (2010), Gaggero et al. (2014), Gaggero and Villa, (2016c). For open water simulations, by exploiting the axial symmetry of propeller and inflow, only a blade passage has been modeled, for a total of about 1.2 million cells per blade and an average non-dimensional wall distance of 150 to fully exploit the realizable k-epsilon wall functions. A snapshot of the resulting mesh and of the refining regions in inclined shaft conditions, where sliding meshes were set to allow the motion of the inner propeller region with respect to the outer domain, is shown in Figure 3.

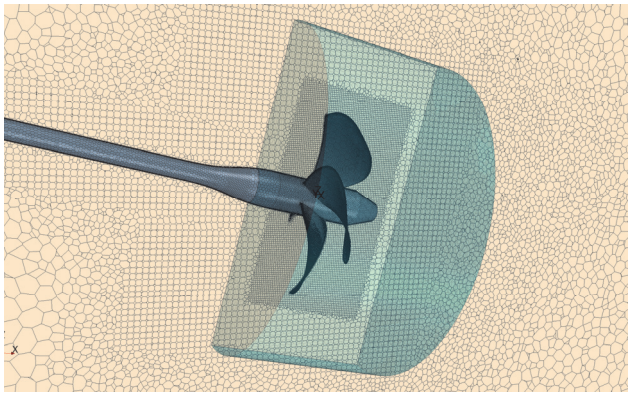

Figure 3: Mesh arrangement for RANSE calculations. Reference propeller in inclined shaft.

In order to perform calculations with an acceptable Courant number, an equivalent time step of 3° was assumed for the non-cavitating simulations. The inclusion of cavitation modeled with the Volume of Fluid approach within the homogeneous mixture approximation and the Schnerr-Sauer mass transfer model (Schnerr and Sauer 2001), required a further refinement of the time step, which was set up equivalent to 0.5°.

3.2 Parametric Description of the Propeller Geometry

The shape of a propeller blade is traditionally described by curves that represent the most significant distributions (pitch, chord, maximum camber, thickness, among the others) from root to tip. Such representation is inherently parametric and may be directly used for the automatic generation of the geometries to be analyzed within the optimization process. Fairness and smoothness are the principal requirements of the description. Among the others, Vestig et al. (2016), proposed an optimization design where the geometry was controlled by parametrically describing distribution curves that manage loading (rather than pitch and camber) or local thickness reductions. In the present work, instead, a more classical modification of the geometrical distributions of the propeller, described with B-Spline curves, as deeply discussed in Bertetta et al. (2012) or in Gaggero et al. (2016a, 2016b) was preferred. The limited number of control points of these curves turn into the free parameters of the optimization, reducing the number of decision variables but still allowing for complex geometry

variations and facilitating the fairness of the shapes. Similarly also local variations of the sectional profiles of the blade may be included in the design process thanks to an identical description of the chordwise distributions of sectional thickness and camber.

In the present case, a set of 48 free parameters was selected to alter the reference propeller geometry. The ranges of variation were selected to balance the need of exploring unconventional shapes and combinations with the need to avoid unrealistic performance improvements due to unfeasible shapes that results from the lack of physics in the medium-fidelity code represented by the BEM. This choice consists in:

- 7 parameters to describe the chord distribution,
- 8 parameters to describe the sectional pitch distribution,
- 9 parameters to describe the maximum camber distribution,
- 12 parameters to describe the B-surface that represents the non-dimensional camber surface of the blade,
- 12 parameters to describe the B-surface that represents the non-dimensional thickness surface of the blade.

3.3 Constraints and Objectives

Optimization is inherently a multi-objective process and, being the design of a propeller always a trade-off between competing objectives and constraints (basically maximize the efficiency with avoidance of cavitation, assuring sufficient blade strength, as explained in the following), the Pareto convergence among which select the best compromise can be better addressed if all requirements and constraints can be turned into parameters and outputs that the codes adopted for the design may accurately evaluate.

With the exception of the geometrical constraints represented by the limits forced for the free variables and hard-coded in the design space, the only other two constraints accepted in the proposed design process regard the blade strength and the maximum speed achievable by the ship.

Any change of chord and pitch results in a change of the load and, in turn, of the functioning point of the propeller. The thickness distribution, therefore, is not free to change independently. A minimum sectional thickness, further corrected to comply with classification rules (RINA, 2015), is derived for any design by approximating the blade to a beam, subjected to the actual thrust and torque (Conolly, 1974), rigidly fixed at the root.

The second constraint concerns the operative conditions of the propeller. In general any new design has to assure a ship speed as close as possible to the reference geometry and forcing a certain delivered thrust for the geometries defined by the optimization fixes this operative point. The fulfilment of an equality constraint, however, is a serious bottleneck for the design process, even if certain margins were accepted to avoid an excessive number of unfeasible geometries and speed up the convergence process. To overcome this limitation, in the present work, a different approach has been adopted, converting the thrust constraint into a couple of objectives: instead than requiring a given thrust, the new propellers have been designed in order to maximize the boat speed exploiting the engine at the Maximum Continuous Rate. The type of the analyzed boat, obviously, allows for this change, being the increase of the maximum cruise speed always an added value for the customer. The optimization workflow requires, consequently, specific procedures. For each geometry, it is necessary to evaluate the correlation between rate of revolution, required power and maximum achievable speed (possible by assuming unchanged the propulsive coefficient measured during a self-propulsion test for the reference propeller) that turn into an objective to be maximized. At the same time, once the matching between the engine layout and the required power curve is performed, minimization is required for the "distance" of the predicted propulsive point from the MCR (as schematically indicated in Figure 4). At the resulting maximum and endurance ship speeds, the risk of cavitation is also evaluated and assumed as a further set of design objectives. Avoidance (or limitation) of cavitation is, in fact, one of the main objectives of the propeller design in order to mitigate the side effects (erosive phenomena, degradation of performance, radiated noise and induced pressure pulses) particularly annoying in the case of high speed crafts.

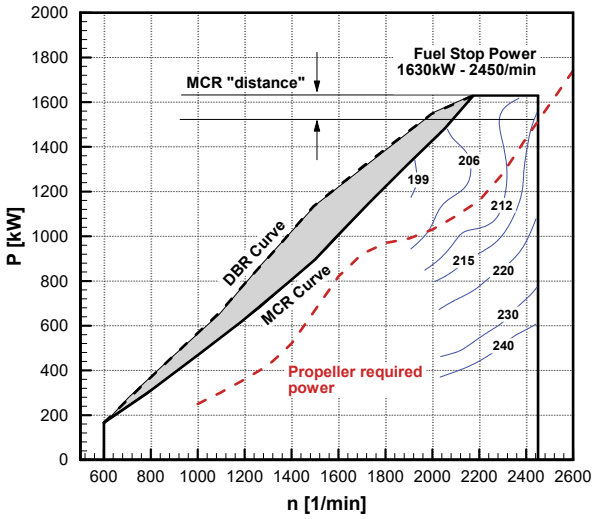

Figure 4: MTU 16V 2000M84 Engine layout and required propeller power (schematic drawing). Maximum speed and minimum distance from the Maximum Continuous Rate are the additional objectives of the design.

Computational efficiency is the key point of the design by optimization and simplified calculations and design criteria are of fundamental importance when thousands of geometries have to be tested in different functioning conditions. The design proposed in this work is based on rather crude assumption (whose reliability however has been accurately verified in the case of the reference propeller) that anyhow closely resemble well-established design procedures (Grossi, 1980) but included in a completely automatic design environment. Non-cavitating analyses were preferred, even if in previous optimization activities the use of the cavitating model with the BEM

provided successful results (Bertetta et al., 2012, Gaggero et al., 2016a, 2016b).

Quasi-steady analyses with radially varying inflow in correspondence of few critical positions inside the hull wake preliminary computed with RANSE (90° and 270° blade position for loaded and unloaded conditions respectively plus the average inflow), furthermore approximated the unsteady behavior of the propeller in inclined shaft, following the successful application of this approximation of Bertetta et al. (2012).

The risk and the possible margins against cavitation can be monitored by using the simplest criterion on pressure ($-C_{PN}<\sigma_N$) for any points on the blade with a single non-cavitating calculation. Tthe type of cavitation (sheet or bubble) can be marked by the position, along the section chord, in correspondence to which the dynamic pressure falls below the vapor pressure. Especially for what regards bubble cavitation, as already mentioned, a simple avoidance criterion based on the minimum of the pressure distributions may result more computationally robust. In addition, the expected extension of the cavitating region, within non-cavitating analyses can be controlled by the combination of two criteria: the portion of the pressure diagram below the vapor pressure (herewith addressed as "inception area", being the region were cavitation for sure starts and occurs) and the strength of the suction peak. Larger zones of "inception area" with higher suction peaks (as per Figure 5) are a symptom of more extended cavitation bubbles that, consequently, can be handled in the design process by requiring their minimization. A combination of the two, a kind of "inception volume", may be considered as a measure of the cavitation strength.

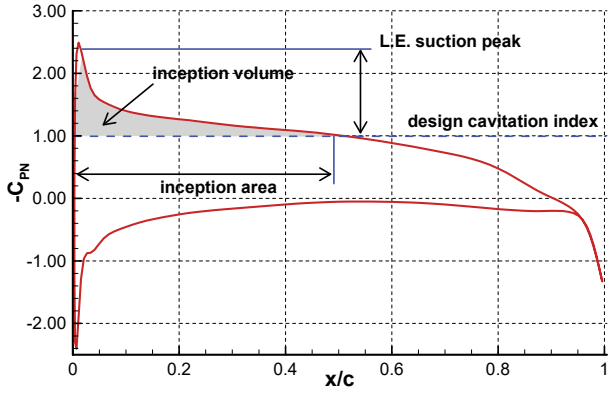

Figure 5: Monitors of the cavitating behavior of each propeller blade radial section: "inception area", "inception volume" and pressure suction peaks.

The design of the new propeller based on these simplified assumptions was carried out by requiring:

1. Set of objectives concerning the craft performance:
   - Maximization of the boat speed at the maximum delivered power,
   - Minimization of the distance of the working point from the engine maximum continuous rate point,
   - Maximization of the propeller efficiency at the endurance speed (70% MCR)
2. Set of objectives concerning the propeller performance at maximum delivered power/speed:
   - Minimization of the cavitation "inception area" on the suction side - equivalent flow at 90° blade position,
   - Minimization of the cavitation "inception area" on the pressure side - equivalent flow at 270° blade position,
   - Minimization of the "inception volume" on the suction side - equivalent flow at 90° blade position,
   - Minimization of the "inception volume" on the pressure side - equivalent flow at 270° blade position,
   - Minimization of the leading edge suction pressure peak coefficient for any blade sections at the tip ($r/R > 0.7$)
   - Minimization of the leading edge suction pressure peak coefficient for any blade sections at inner radii ($r/R < 0.7$)
   - Minimization of the midchord suction pressure peak coefficient for any blade sections
3. Set of objectives concerning the propeller performance at endurance speed:
   - Minimization of the cavitation "inception area" on the suction side - equivalent mean inflow
   - Minimization of the "inception volume" on the suction side - equivalent mean inflow

In addition, also the inception areas on the pressure side at maximum speed at the loaded condition (90°), on the suction side at maximum speed at the unloaded condition (270°) and on the pressure side at the endurance speed for the average flow were monitored and all the geometries that showed any of these issues were discarded during the post-processing of the results.

3.4 Optimization Final Workflow

By combining the above mentioned parametric description of the geometry, the appropriate flow solvers and by selecting objectives and constraints, the design by optimization can be seen as an automatic "trial and error" procedure, that in present case is driven to convergence by using a multi-objective genetic type optimization algorithm within the ModeFRONTIER software environment (Esteco, 2014). The design of the optimal geometry is indirect, rising from the analysis of hundreds (thousands) of different possible configurations among which the better candidates against the selected constraints and objectives may be identified.

Due to the large amount of free parameters and objectives it was necessary to select an initial populations sufficiently wide (1500 members) to reasonably cover the design space and let it evolve for 35 generations to achieve a satisfactory Pareto convergence. BEM, for these reasons, results as the only possible medium-fidelity computational approach to be employed for the evaluation of the about 50000 geometries iteratively defined by the optimization algorithm in a time (about 7 days on a common workstation) compatible with the usual design process. RANSE calculations, as shown in the flow chart that summarizes the design process of Figure 6, was adopted only a posteriori for a reanalysis of a set of Pareto

configurations (including inclined shaft calculations with cavitation) among which identify, on the basis of further detailed high-fidelity analyses, the optimal geometry.

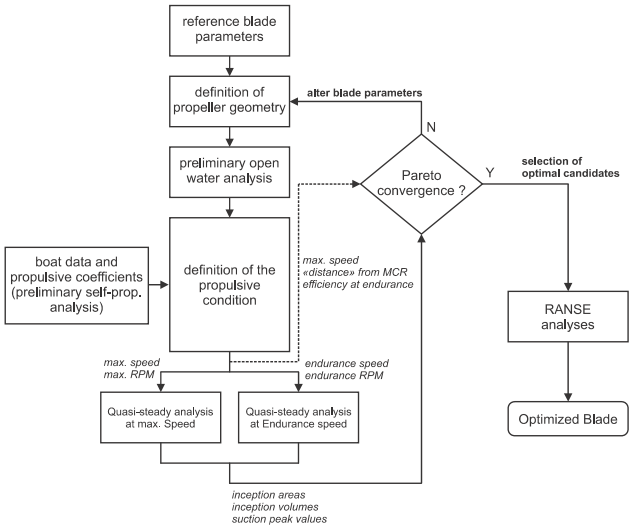

Figure 6: workflow of the design process based on optimization.

4 VALIDATION OF THE DESIGN TOOLS

Validation is a crucial step for a reliable and accurate design. The original design, a five blade, fixed pitch propeller, is already characterized by very high performance that makes the optimization process very challenging. The preliminary analysis, as usual, serves to validate the design tools, provide useful information circa the possible issues of the reference design in order to guide the optimization design and calibrate the process to achieve reliable results. In addition, a comparison with observations and calculations (both BEM and RANSE) with resolved cavitation is mandatory to assess the applicability of the simplified criteria ("inception area" and pressure suction peaks) to monitor the risk of cavitation.

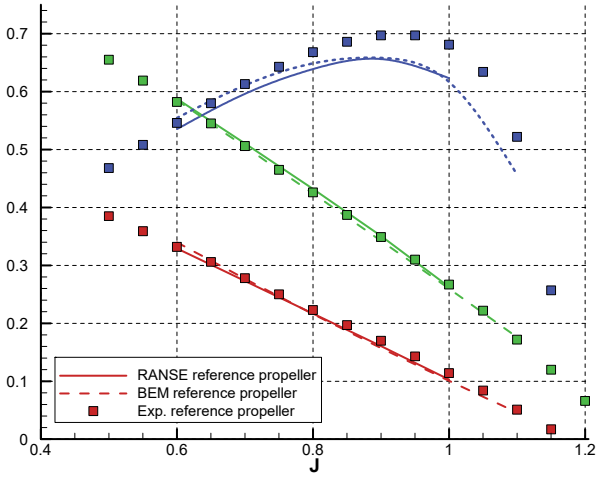

Figure 7: Comparison among measurements, BEM and RANSE calculations in open water conditions for the reference propeller.

As expected the agreement between measurements and calculations in open water conditions (Figure 7) is good. With respect to measurements, forces predicted by the Boundary Elements Method are slightly underestimated, in particular for unloaded conditions. Close to the design advance coefficient (about J = 0.8) the underestimation is of 3% for thrust and 0.5% for torque. High-fidelity RANSE results are slightly better. At the design point, thrust and torque are 2.5% under- and 0.5% overestimated respectively. By assuming that the same numerical issues will affect each new geometry derived by means of small geometrical modifications of the reference propeller, a calibration of BEM results based on RANSE results was accepted for the prediction of the functioning conditions of any propeller analyzed in the design process. The prediction of cavitation and of the inception area in uniform inflow with BEM and RANSE at the design cavitation index (σ_N= 0.85) is summarized in Figures 8, 9, 10 and 11. Advance coefficients equal to 0.7, 0.8 and 0.9 were selected to include, by means only of uniform inflow calculations, all the possible blade sections working conditions.

With the cavitation models of both the BEM and the RANSE it is not possible to discern between sheet and bubble cavitation and the presence of bubbles at midchord is approximated with a continuous, very thin, sheet vapor bubble over almost all the blade suction side (loaded condition, J = 0.7). At J = 0.8, the agreement between RANSE and BEM is satisfactory and the predicted spots of vapor in the tip region close to the trailing edge are well in agreement with the observations.

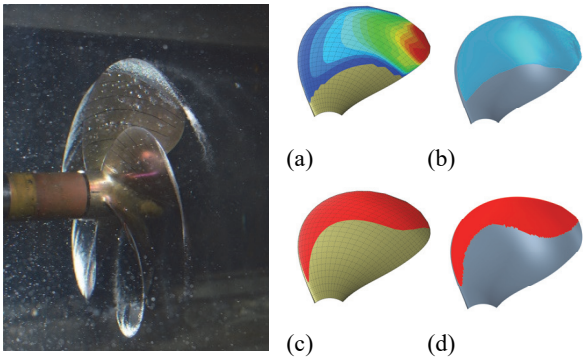

Figure 8: Cavitation tunnel observation (J = 0.7, suction side, σ_N= 0.85) and (a) BEM (cavitating), (b) RANSE (cavitating), (c) BEM (inception area) and (d) RANSE (inception area).

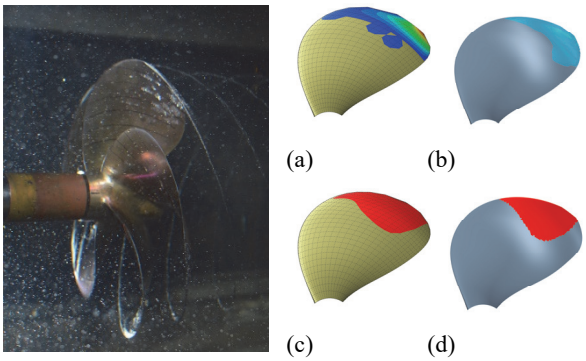

Figure 9: Cavitation tunnel observation (J = 0.8, suction side, σ_N= 0.85) and (a) BEM (cavitating), (b) RANSE (cavitating), (c) BEM (inception area) and (d) RANSE (inception area).

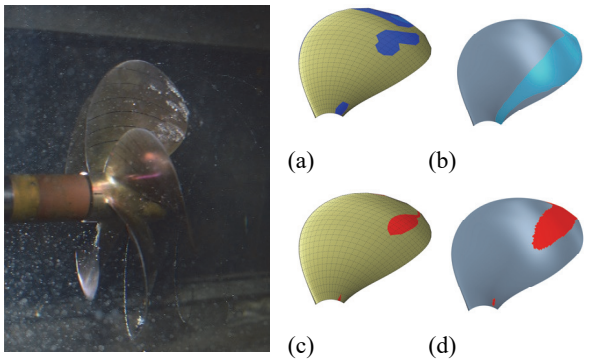

Figure 10: Cavitation tunnel observation (J = 0.9, suction side, σ_N= 0.85) and (a) BEM (cavitating), (b) RANSE (cavitating), (c) BEM (inception area) and (d) RANSE (inception area).

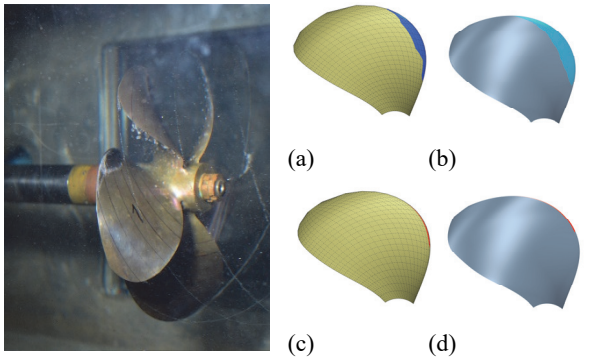

Figure 11: Cavitation tunnel observation (J = 0.9, pressure side, σ_N= 0.85) and (a) BEM (cavitating), (b) RANSE (cavitating), (c) BEM (inception area) and (d) RANSE (inception area).

In lightly loaded condition (J = 0.9) also BEM foresees midchord bubbles that however underestimate the radial extension observed during measurements and reasonably evidenced by RANSE. Furthermore, pressure side cavitation at leading edge, observed at J = 0.9, is similarly predicted by the two numerical approaches. Also the "inception areas" by both the approaches reasonably foresee these features, confirming a positive correlation of the phenomena (inception area criterion, fully developed bubble and, more importantly, observations) to be exploited in the design by optimization process. The large area where the pressure coefficient is below the design cavitation index persists, at midchord near the tip, also when the local angle of attack is reduced. This is a symptom of "flat" pressure diagrams at the design point that underline the risk of bubble cavitation (observed and approximated by the cavitation models) which may represent a possible margin of improvement of an already well designed propeller. Both the chordwise and the radial extensions of the inception areas underestimate the presence of cavitation, whose "true" extension (as shown by the calculations with cavitation enabled) is, of course, significantly affected by the development of the bubble itself. The analysis proves, anyhow, that the simpler non-cavitating pressure distributions can fairly serve as an indicator of the different types of cavitation and of their risk of occurrence in the design process.

5 RESULTS OF THE OPTIMIZATION PROCESS

The preliminary analysis of the reference propeller confirms the complexity of the design of highly-loaded high speed propellers. Margins for the improvement of the cavitating performance are rather limited with almost "shock-free" pressure diagrams at the design point. A change in the rake distribution to unload the tip (Dang, 2004, Gaggero et al. 2016b) could increase cavitation margins at tip. On the other hand, the required maximization of the boat speed turns into a differently distributed load with a decrease of efficiency and an increased risk of sheet cavitation at intermediate radial positions that the optimization process has to mitigate.

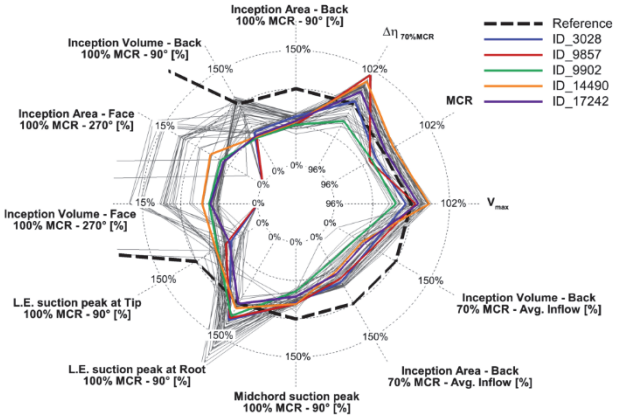

Figure 12: Pareto diagram sub-selection.

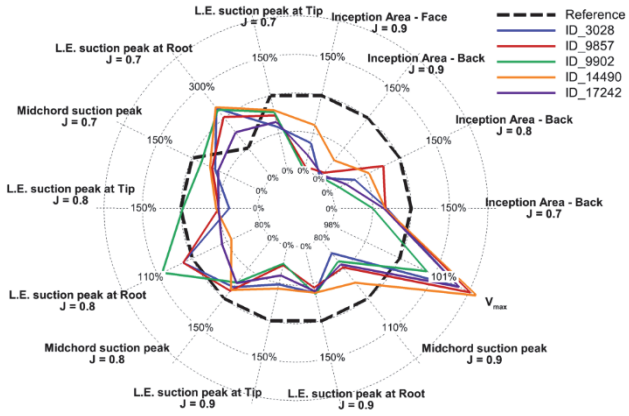

Figure 13: RANSE performance for the selected geometries.

A summary of the most significant geometries identified by the design process based on BEM is shown in Figure 12. Among these, five (ID_3028, ID_9857, ID_9902, ID_14490 and ID_17242) have been selected for further RANSE analyses, whose results are summarized in Figure 13. Only a selection of the design objectives identified in Section 3.3 has been included in the representation of results.

The effectiveness of the design process is remarkable. The unloading of the blade due to rake distribution determines a consistent reduction, among the Pareto designs and in particular for the selected geometries, of the inception area at the maximum loading in correspondence to the 90° blade position. Also the suction peak at tip is significantly lowered as a symptom of retarded inception, as well as the inception area on the pressure side with few geometries

even succeed in completely avoiding face cavitation. These improvements, obviously, have some costs. As a result of the redistribution of load induced by the different rake distribution and the simultaneous maximization of the boat speed and propeller efficiency (that on the basis of BEM calculations increased up to 1.5% and 2% respectively), the suction peak at on blade sections close to root is higher with a consequent increased risk of sheet cavitation. These results by the Boundary Elements Method are completely confirmed by the RANSE. The reduction of the inception area at any working conditions evidenced by the BEM in the optimization process is exactly computed when viscous calculation in "equivalent" uniform inflow (J=0.7 instead of 90° blade position, J=0.8 instead of average inflow and J=0.9 instead of 270° blade position) are considered. For all the five geometries under analysis, the improvements in terms of extension of the region with a pressure below the vapor one are remarkable and he inception points at different loading have been successfully postponed. Only the suction peak at root in the loaded condition (J = 0.7) is significantly higher than the reference propeller, as anticipated by the Boundary Elements Method analyses; this has been voluntarily accepted since focus of optimization is the elimination of midchord bubbles. ID_17242, based on BEM and RANSE preliminary calculations, provides a significant reduction of the cavity extension with the overall better performance in terms of postponing of the cavity inception (at loaded and design conditions), with the exception of the unloaded condition where ID 14490 and ID 3028 perform slightly better. For these reasons, it was selected for detailed numerical analyses and dedicated cavitation tunnel observations, as well as full-scale surveys.

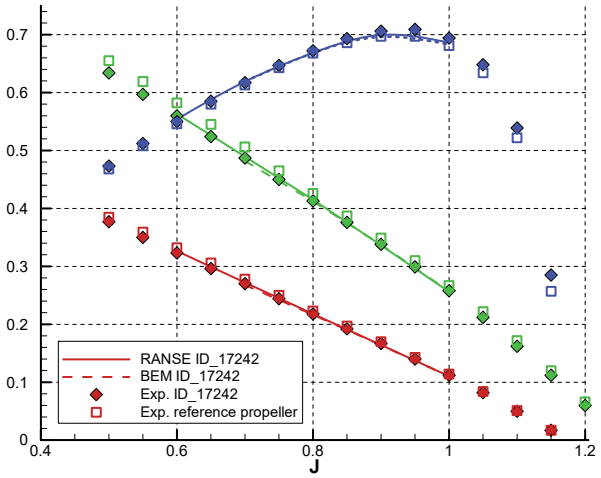

Figure 14: Measurements, BEM and RANSE calculations in open water conditions for the ID_17242 propeller. Comparison with measured thrust and torque of the reference propeller.

The comparison between towing tank tests and numerical calculations of Figure 14 confirms, in addition to the analyses carried out for the reference propeller, the reliability of both the BEM and the RANSE approaches. For the whole range of advance coefficients under investigation, the accuracy of both calculations is even higher than that observed in the case of the reference geometry, in particular for what regards the Boundary Elements Method, which in general suffers rake distributions excessively pointing towards the suction side, as that of the reference propeller. Close to the design point, around J = 0.8, the error with respect to measurements is lower than 0.5%: this, in turn, should imply the reliability of the maximum craft speed prediction, within the assumed hypotheses of invariance of the propulsive coefficients as a consequence of a different propeller geometry. Measurements show a slight increase of the propeller efficiency that even in the simpler case of open water conditions is in line with outcomes of the numerical calculations carried out for the optimization.

RANSE predictions of the inception areas at the three advance coefficients representative of loaded, design and unloaded functioning of the propeller operating in inclined are shown in Figure 15.

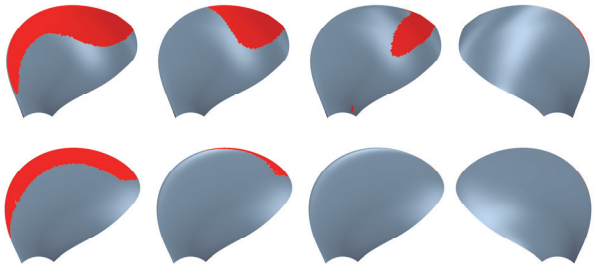

Figure 15: Comparison of the "inception areas" at the design cavitation index σ_N= 0.8463. Reference propeller (top) and ID 17242 (bottom). J = 0.7, 0.8, 0.9 and 0.9 pressure side.

Even if the inception point is slightly postponed, the optimized propeller still shows a consistent risk of leading edge sheet cavitation at J = 0.7, as expected by the unloading of the tip and the radial redistribution of load. As expected, the ID 17242 however delivers its best performance close to the design point and in unloaded conditions. At J = 0.8 the risk of cavitation is limited to the tip of the blade with a certain margin against bubble cavitation anywhere else on the blade. In correspondence to the unloaded condition, the suction side is completely free of cavitation: on the pressure side only few sections are subjected pressure below the vapor limit, the inception is postponed and a non-negligible margin protects from midchord bubble cavitation. RANSE calculations in inclined shaft with cavitation (Figure 16) recognize the different cavitating behavior of the propellers. The thickness of the cavity bubble is significantly reduced as reduced is its extension and location. At 90° blade position, cavitation is predicted as a sheet cavity bubble from leading edge (in accordance with the resulting modified shape of the pressure diagrams) with a substantial reduction of the phenomena regarding midchord and, as foreseen by the previous analyses, pressure side cavitation is almost nullified.

These results are furthermore sustained by the experimental observations proposed in Figure 17. As expected, bubble cavitation is significantly reduced. Only

at 90° the optimized propeller shows some midchord bubbles that are, however, far from the extension observed on the reference blade and in accordance with the outcomes of the design process.

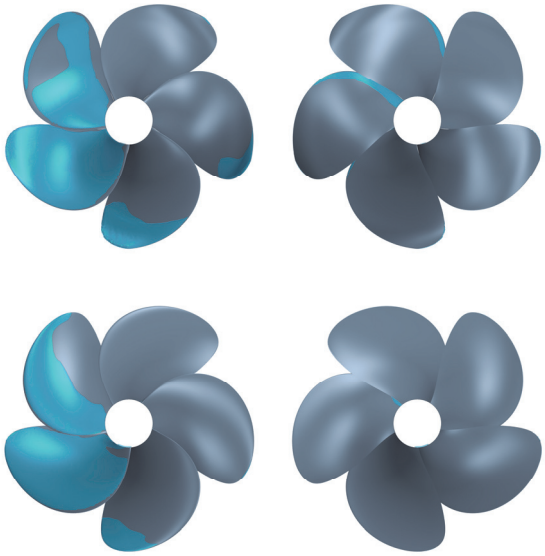

Figure 16: Predicted unsteady cavitation (inclined shaft) using RANSE at the design cavitation index. On the top: reference propeller suction (left) and pressure side (right). On the bottom: ID_17242 propeller suction (left) and pressure side (right). Key-blade at 0° position.

The agreement of the numerical calculations of Figure 16 is only qualitative due to the limitations of the homogenous mixture. The absence of sheet cavitation on the pressure side in the case of the optimized propeller proves the reliability of the numerical calculations. Cavitation inception points are summarized and compared in Figures 18 and 19 for sheet/vortex and bubble phenomena respectively. The optimized propeller shows substantial improvements for any of the phenomena observed with the exception of bubble cavitation at root in correspondence to the 270° position that is a further proof, by comparing the Pareto diagrams of Figure 12 and 13, of the reliability of the criteria adopted during the optimization. The reduction of cavitation positively influences also the delivered thrust. With respect to the reference geometry, the optimized propeller has an almost negligible thrust breakdown in cavitating conditions that may balance the less effective role of the pressure side rake in achieving higher efficiency. Numerical calculations (both BEM and RANSE) mainly overestimate the reduction of thrust in cavitating conditions. This is particularly true in the case of the reference propeller for which, however, the peculiarity of the cavitating phenomena dominated by midchord bubbles, may represent a valid explanation of the poor performance of cavitating models not completely suited for these conditions. Trends, which are qualitatively in agreement with measurements, still confirm the effectiveness of the design by optimization.

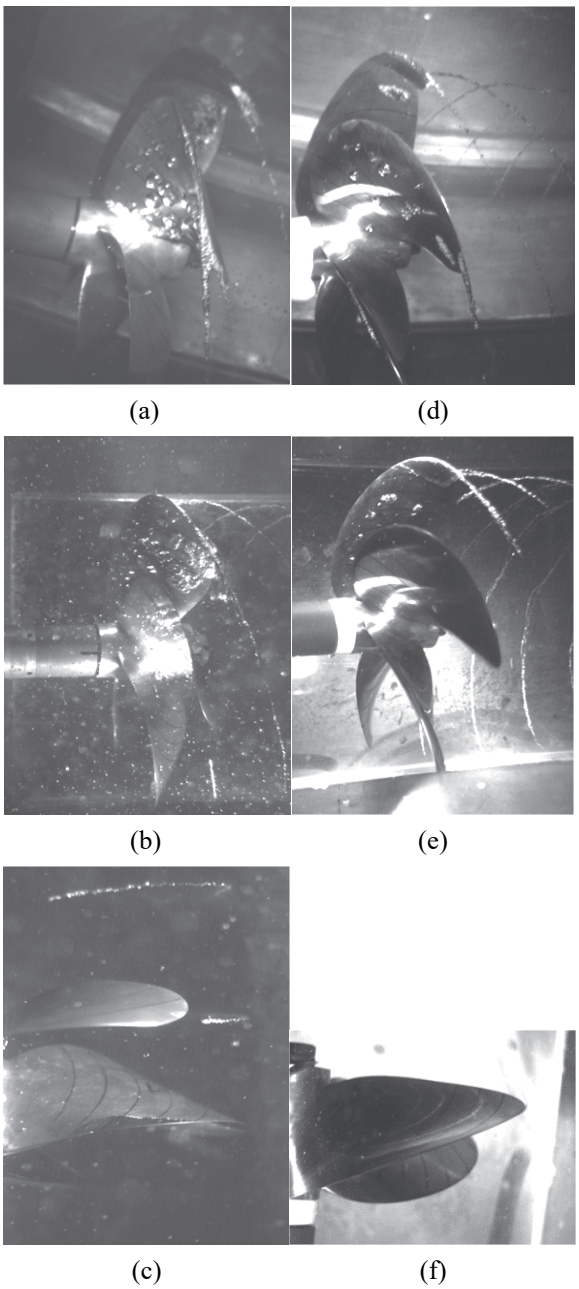

Figure 17: Cavitation observations. Reference propeller: (a) suction side at 90° from starboard, (b) view from above and (c) pressure side at 270°. Optimized ID_17242 propeller: (d) suction side at 90° from starboard, (e) view from above and (f) pressure side at 270°.

These results were achieved, as exemplified in Figure 20, by a radical modification of the relevant distributions along the radius. In addition to a modification of the rake (from suction to pressure side), the optimal propeller presents a substantial increase of the expanded area. Chord is everywhere higher: combined with a reduction of camber it simultaneously avoids suction peaks at the leading edge and the risk of excessive suction (i.e. bubble cavitation) at midchord. The unloading resulting from the modified rake is balanced, further by the increase of the blade area, by a more loaded pitch distribution.

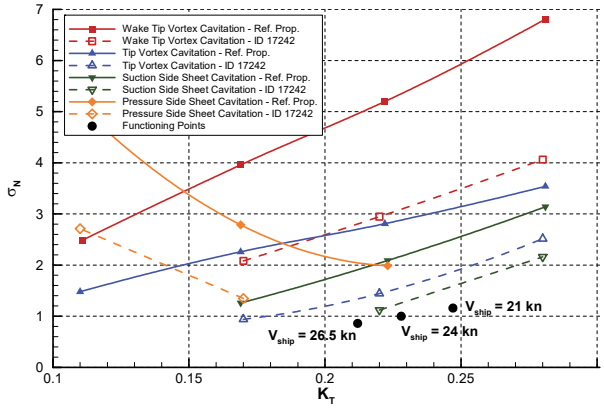

Figure 18: Comparison of the experimental inception point of vortex and sheet cavitation.

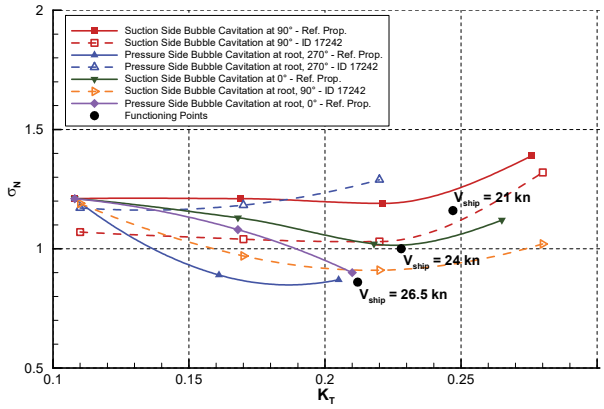

Figure 19: Comparison of the experimental inception point of bubble phenomena.

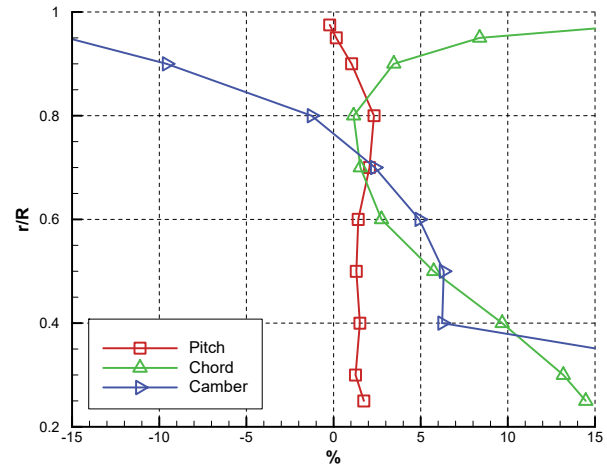

Figure 20: Comparison between reference and optimized propeller geometries. Non-dimensional values based on local quantities of the reference geometry.

The reliability of the design and the consistency of the improvements foreseen by the optimization was finally verified by the dedicated comparative sea trials (on the same boat). Results, summarized in Table 4, show the measured ship speed in two runs (in opposite direction, as common practice). For each run, the average propeller rate of revolution (as a percentage of the maximum) is reported for each shaft, together with the resultant boat speed. In all cases, the maximum engine power was delivered to the propellers. The propeller rate of revolution is a good parameter to define the expected distance of the working condition from the objective, showing a better overall matching (even if propeller behavior was not symmetrical) of the optimized geometry with respect to the reference propeller. This result confirms the overall reliability of the optimization tools and of the current implementation of the design constraints. In addition, it represents together with the increase of the maximum boat speed, an important indicator of the effectiveness of the proposed design procedure. The increase of 1 kn is higher than that predicted during the optimization using BEM (+0.25kn) and in the post-processing of the selected geometries using RANSE (+0.5kn). These differences, further to the uncertainties of measurements (ship loading condition and sea state were not exactly the same), could also be explained by the approximate inclusion of the actual thrust breakdown in the design process by using quasi-steady BEM analyses that only the final RANSE calculations can reasonably predict. This can be considered as one of the key point still open for an even more robust automatic and computationally efficient design process.

Table 3: Propellers performance in inclined shaft condition.

Reference propeller		Non Cav.	Cav.	
RANSE	K_T	0.2224	0.1981	-10.9%
	$10K_Q$	0.4221	0.3870	-8.5%
BEM	K_T	0.2096	0.2004	-4.4%
	$10K_Q$	0.3974	0.3917	-1.4%
Exp.	K_T	0.223	0.210	-5.7%
	$10K_Q$	0.438	0.417	-4.8%
ID_17242		Non Cav.	Cav.	
RANSE	K_T	0.2186	0.2141	-2.09%
	$10K_Q$	0.4187	0.4131	-1.34%
BEM	K_T	0.2142	0.2093	-2.3%
	$10K_Q$	0.4044	0.4029	-0.4%
Exp.	K_T	0.213	0.212	-0.4%
	$10K_Q$	0.414	0.412	-0.3%

6 CONCLUSIONS

In the present paper, a design by optimization process, based on genetic algorithm and BEM calculations, has been proposed and validated by using dedicated model scale measurements and sea trials for a high-speed propeller. The devised procedure relies on some simplifications (inception area concept and quasi-steady calculations, need of day affordable designs) whose effectiveness has been analyzed considering viscous computations and, preliminarily for the reference propeller, also experimental measurements.

Suitable formulations of the optimization objectives and constraints have been, consequently adopted. An explicit blade strength estimation has been included in the process, together with an engine – propeller matching algorithm to derive the functioning conditions of each geometry defined by the optimization and to change usual thwarting constraints circa the delivered thrust into design objectives.

Table 4: Sea trials results at 100% of the delivered power.

		Max. Speed [kn]	Propeller Rate of Revolution [% MCR]	
			Left Shaft	Right Shaft
Reference Propeller	Run 1	26	98.9%	98.3%
	Run 2	25.3	98.7%	98.7%
	Average	25.7	98.8%	98.5%
ID_17242	Run 1	26.2	98.7%	99.9%
	Run 2	27.1	98.9%	100.0%
	Average	26.7	98.8%	100.0%

After the analysis of the Pareto candidates and additional high-fidelity RANSE calculations on a rationally selected subset of geometries, an optimal propeller was identified. Model scale experiments largely confirmed the reliability of the design tools for what regards both the prediction of propeller characteristics and the estimation of cavitation as well: efficiency is higher and cavitation sensibly reduced. From this point of view, cavitation tunnel experiments furthermore clarified the bubbly nature of most of the suction side cavitation phenomena predicted in the form of sheet cavitation by both the numerical methods due to the inherent limitations of the cavitating models. The easier analysis of non-cavitating pressure distributions turns out to be, consequently, a valid simplification to be exploited in the design process.

Sea trials surveys, finally, confirmed the overall reliability of the tools employed in the optimization and, even if accounting for the small differences between the two crafts equipped with the propellers, they still represent an important indication of the effectiveness of the proposed design procedure. The need of more accurate predictions of thrust breakdown due to cavitation results, on the other hand, as a mandatory aspect for an even more robust automatic and computationally efficient design process.

REFERENCES

Bertetta, D., Brizzolara, S., Gaggero, S., Savio, S. & Viviani, M. (2012). 'CPP propeller cavitation and noise optimization at different pitches with panel code and validation by cavitation tunnel measurements', Ocean Engineering, **53**, pp. 177-195.

Betz, A. (1927). 'Schraubenpropeller mit geringstem Energieverlust', Vier Abhandlungen zur Hydrodynamik und Aerodynamik, pp. 68-92.

Brizzolara, S., Villa, D. & Gaggero, S. (2008). 'A systematic comparison between RANS and Panel Methods for Propeller Analysis', Proceeding of 8th International Conference on Hydrodynamics ICHD2008, Nantes France.

Brizzolara S., Gaggero S. & Grassi D. (2013). 'Hub Effect in Propeller Design and Analysis', Third International Symposium on Marine Propulsors, smp2013, Launceston, Tasmania, Australia.

Brizzolara S., Grassi D. & Tincani E.P. (2012). 'Design Method for Contra-Rotating Propellers for High- Speed Crafts: Revising the Original Lerbs Theory in a Modern Perspective', International Journal of Rotating Machinery.

Brockett, T.E. (1966). 'Minimum Pressure Envelopes for Modified NACA-66 Sections with NACA a=0.8 Camber and Buships Type I and Type II Sections', DTMB Report 1780, Carderock, MD.

CD-Adapco (2012). 'Star-CCM+ 7.04.006 Users Guide'.

Coney, W. B. (1989). 'A Method for the Design of a Class of Optimum Marine Propulsors', PhD thesis, Massachusetts Institute of Technology.

Conolly, J. E. (1974). 'Strength of propellers', Transactions of Royal Institutions of Naval Architects, **103**, pp. 139 – 204.

Dang, J. (2004). 'Improving Cavitation Performance with New Blade Sections for Marine Propellers', International Shipbuilding progress, **51**(4), pp. 353 – 376.

Diniz, G. & Brizzolara, S. (2015), 'Fully Numerical Lifting Line Method for Propeller Design', Proceedings of the Fourth International Symposium on Marine Propulsors, smp2015, Austin, Texas, USA.

Epps, B., Víquez, O. & Chryssostomidis, C. (2011). 'Dual-Operating-Point blade optimization of high-speed propellers', 11th International Conference on Fast Sea Transportation FAST 2011, Honolulu, Hawaii.

Esteco S.r.l. (2014). 'ModeFRONTIER 2014 User's Manual'.

Fine, N.E. (1992). 'Nonlinear Analysis of Cavitating Propellers in Nonuniform Flow', PhD Thesis, Massachusetts Institute of Technology.

Fine, N. E. & Kinnas, S. A. (1993), 'A Boundary-Element Method for the Analysis of the Flow around 3-D Cavitating Hydrofoils', Journal of Ship Research, **37**(3), pp. 213 – 224.

Gaggero S., Rizzo C.M., Tani G. and Viviani M. (2012). 'EFD and CFD design and analysis of a propeller in decelerating duct', International Journal of Rotating Machinery.

Gaggero, S., Gonzalez-Adalid, J. & Perez Sobrino, M. (2016a). 'Design of Contracted and tip loaded propellers by using boundary element methods and optimization algorithms', Applied Ocean Research, **55**, pp. 102 – 129.

Gaggero, S., Gonzalez-Adalid, J. & Perez Sobrino, M. (2016b). 'Design and Analysis of a new generation of CLT propellers', Applied Ocean Research, **59**, pp. 424 – 450.

Gaggero, S. & Villa, D. (2016c). 'Steady cavitating propeller performance by using OpenFOAM, StarCCM+ and a boundary element method', Proc.

IMechE Part M: Journal of Engineering for the Maritime Environment.

Gaggero S., Villa D. & Viviani M. (2014a). 'An investigation on the discrepancies between RANSE and BEM approaches for the prediction of marine propeller unsteady performances in strongly non-homogeneous wakes', ASME 2014 33rd International Conference on Ocean, Offshore and Artic Engineering, OMAE 2014, San Francisco, USA.

Gaggero, S., Villa, D. & Brizzolara, S. (2010). 'RANS and panel methods for unsteady flow propeller analysis', Journal of Hydrodynamics, **22**(5B-1), pp. 547 – 552.

Grossi, L. (1980). 'PESP: un programma integrato per la progettazione di eliche navali con la teoria della superficie portante', CETENA Report n.1022 (in Italian).

Hsin, C.Y. (1990). 'Development and analysis of Panel Methods for Propellers in Unsteady Flows', PhD thesis, Massachusetts Institute of Technology.

Kerwin, J.E., Coney, W.B. and Hsin, C.Y. (1986). 'Optimum circulation distribution for single and multi-component propulsors', Proceedings of Twenty-First American Towing Tank Conference, Washington D.C., USA.

Lerbs, H.W. (1952). 'Moderately loaded Propellers with a Finite Number of Blades and an Arbitrary Distribution of Circulation', SNAME Transactions, **60**, pp. 73 – 117.

Morino, L. & Kuo, C.C. (1974). 'Subsonic Potential Aerodynamic for complex configuration: a general theory', AIAA Journal, **12**, pp. 191 – 197.

Mueller, A.C. & Kinnas, S.A. (1999). 'Propeller sheet cavitation predictions using a panel method', Journal of Fluids Engineering, **121**, pp. 282 – 288.

RINA - Registro Italiano Navale (2013). 'Rules for the Classification of Yachts Designed for Commercial Use', Part C, Chapter 1, Section 7, Effective from 1 January 2013, Registro Italiano Navale, Genoa, Itay.

Schnerr G. & Sauer J. (2001). 'Physical and numerical modeling of unsteady cavitation dynamics', Proceedings of the 4th International Conference on Multiphase Flow, New Orleans, Luisiana, USA.

Vaz, G. (2005). 'Modelling of Sheet Cavitation on Hydrofoils and Marine Propellers using Boundary Element Methods', PhD Thesis, Technical University of Lisbon – IST.

Vesting, F., Gustafsson, R., & Bensow, R. E. (2016). 'Development and application of optimisation algorithms for propeller design', Ship Technology Research, **63**(1), pp. 50 – 6

DISCUSSION

Question from Eckhard Praefke

I noted the two separated design optimization objectives, "max efficiency @ 100%MCR" and "max efficiency @ 70%MCR". My question: what are the methods to achieve propeller open water curves resulting in good (optimum) efficiency simultaneously at two different J-values?

Author's closure

The maximization of the efficiency objectives used in the design process has to be considered in a relative (local) sense. Of course, it is not possible to have simultaneously the maximum of open water efficiency at two different advance coefficients. The design by optimization works in order to create geometries that, further to reduce the extension of the area subjected to cavitation, simultaneously increase the efficiency at the maximum boat speed (100%MCR) and the efficiency at the boat endurance speed (70%MCR) with respect to the performance of the reference propeller at the corresponding advance coefficients. This additional objective represented by the efficiency at 70%MCR is useful, in addition to the experience of the designer who has to select the final geometry form the Pareto set, to have a quantification of the propeller performance in correspondence of the most significant operative points of the boat and to identify balanced configurations.